

## Effect of seepage flow on critical tractive force of cohesionless soil bed subjected to surface flow

Arif Hossain Jewel<sup>1</sup>, K. Fujisawa<sup>1</sup>, and A. Murakami<sup>1</sup><sup>1</sup>Graduate School of Agriculture, Kyoto University, Kitashirakawa-Oiwakecho, Sakyo-ku, Kyoto 606-8502, Japan**ABSTRACT**

Experiment is conducted to investigate injection or upward seepage effects on critical tractive force of cohesionless soil bed which is subjected to surface flow. The upward seepage force acting on the soil bed particles may reduce the virtual weight of the soil particles. Thus it also reduces the critical tractive force acting on soil bed particles. The theoretical analysis examines how the additional seepage force acts to modify the critical tractive force for sediment entrainment due to increase the hydraulic gradient of the seepage flow. Force analyses reveal that the ratio of the critical tractive force with seepage to that without seepage is proportional to the ratio of the hydraulic gradient of seepage to its value at the critical hydraulic gradient. A test apparatus has been built and the effects of injection on the critical tractive force of cohesionless soil bed particles have been measured: an acrylic channel with a rectangular cross section was prepared and a section of a cohesionless soil bed subjected to the upward seepage flow was installed at the bottom of the channel. The experiment demonstrates that the induced seepage affects the dynamics of channel flow, even though the magnitude of the seepage flow velocity is significantly smaller than the magnitude of the free surface water flow. The test results have shown that the critical tractive force of the cohesionless soil bed particles slightly decreases as the hydraulic gradient of the seepage flow increases. However, it does not sharply decrease even when the hydraulic gradient approaches to the critical hydraulic gradient.

**Keywords:** cohesionless soil bed; critical tractive force; injection**1 INTRODUCTION**

The permeable boundaries are often found in natural rivers, banks, irrigation and drainage channels and earthen dams in the form of sand particles and gravels. Streamflow through these structures may interact with groundwater in different ways. For a stream flow to gain water, the elevation of the groundwater table in the vicinity of the stream must be higher than that the stream water surface. In this situation, the process of flowing of water towards stream is known as upward seepage or injection. In most cases, upward seepage velocity within the porous boundary is even smaller than the free stream velocity above the bed. This small flow induces mass and momentum transfer which has a significant influence on the flow characteristics and sediment transport behavior of a channel. If the injection effect is significant enough, the sand particles on the bed may boil. Consequently, it leads to significant bank failure and or rapid bed form change.

Generally, the effect of seepage on sediment particle movement may be divided into three categories, namely, seepage effects on streamwise velocity distribution and bed shear stress, critical tractive force, and sediment transport rate (Liu and Chiew, 2012).

Thus far, the change in velocity profile of the surface flow due to the seepage flow in the permeable bed has

been investigated, and modifications were added to the wall-law, such as the logarithmic law considering the seepage velocity on the bed. Cheng and Chiew (1998), Krogstad and Kourakine (2000), Dey and Nath (2010) conducted the measurement of the velocity profile near the permeable bed with injection and suction. They discussed the seepage effect on the velocity profile and modified the logarithmic law by their measurements.

Different analytical, experimental and numerical models performed by numerous researchers suggest that critical shear stress is reduced in the presence of injection (Dey and Zanke, 2004). On the other hand, Kavcar and Wright (2009) show that the critical shear stress is decreased with injection but increased with suction. Since seepage adds additional force to the bed, it might have an impact on the sediment transport rate of a channel. Some studies suggest that injection increases bed erosion while other show an opposite result, stating that suction increases sediment transport rate and injection inhibits the motion of bed particles (Lu et al.2008).

Results reported so far are not conclusive enough to understand this complex effects qualitatively and can be contradictory to one another. Hence, there appears the necessity to undertake further investigations. The purpose of this study is the determination of the critical tractive force of cohesionless soil bed particles, subjected to upward seepage flow with the different

hydraulic gradients.

### 1.1 Critical tractive force

The critical tractive force in the absence of seepage flow is non-dimensionalized as follows

$$\tau_c^* = \frac{\tau_c}{(\rho_s - \rho_w)dg} \quad (1)$$

where  $\tau_c^*$ ,  $\tau_c$ ,  $\rho_s$ ,  $\rho_w$ ,  $d$ , and  $g$  denote the dimensionless critical tractive force, the critical tractive force with the dimension of stress, grain density, water density, the diameter of cohesionless soil particles, and gravitational acceleration, respectively. When the permeable bed has the injection, the following magnitude of seepage force,  $f$  additionally acts to each particle of the bed material in the upward direction,

$$f = \frac{\rho_w g i}{(1-n)} \quad (2)$$

where  $i$  and  $n$  denote hydraulic gradient and porosity, respectively. Assuming that the ratio of Eq. (1) maintains even when the bed is subjected to the upward seepage flow on the incipient motion of the particle, the following relation can be derived.

$$\frac{\tau_{cs}}{(\rho_s - \rho_w)dg - fd} = \frac{\tau_c}{(\rho_s - \rho_w)dg} \quad (3)$$

where  $\tau_{cs}$  denotes the critical tractive force under the upward seepage flow. Substituting Eq. (2) into Eq. (3) and Eq. (3) is reduced into the following relation,

$$\frac{\tau_{cs}^*}{\tau_c^*} = \frac{\tau_{cs}}{\tau_c} = 1 - c \frac{i}{i_c} \quad (4)$$

However, according to Martin and Aral (1971), the soil grains on the bed surface experiences seepage force roughly half as large as the soil grains several layers

thick. Thus, we assume that a factor of  $c \approx 0.5$  reduces the seepage force; therefore

$$\frac{\tau_{cs}^*}{\tau_c^*} = \frac{\tau_{cs}}{\tau_c} = 1 - c \frac{i}{i_c} \quad (5)$$

where  $i_c$  is the well-known critical hydraulic gradient, and  $\tau_{cs}^*$  is the dimensionless critical tractive force of  $\tau_{cs}$  shown below.

$$i_c = (1-n) \left( \frac{\rho_s}{\rho_w} - 1 \right), \tau_{cs}^* = \frac{\tau_{cs}}{(\rho_s - \rho_w)dg} \quad (6)$$

Chen and Chiew (1999) and Liu and Chiew (2012) have derived the same Equation as Eq. (4) considering the balance of the forces exerted onto a sediment particle. The relationship between the dimensionless critical tractive force and the hydraulic gradient of Eqs. (4) and (5) is shown as the solid and dash line in Fig. 1.

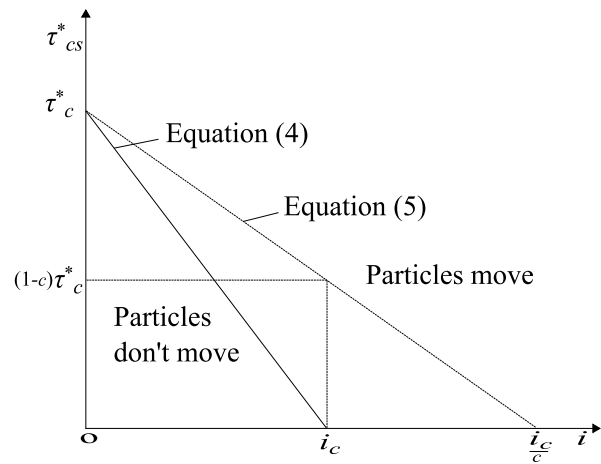


Fig. 1. Conceptual relation of dimensionless critical tractive force and hydraulic gradient.

## 2 EXPERIMENT

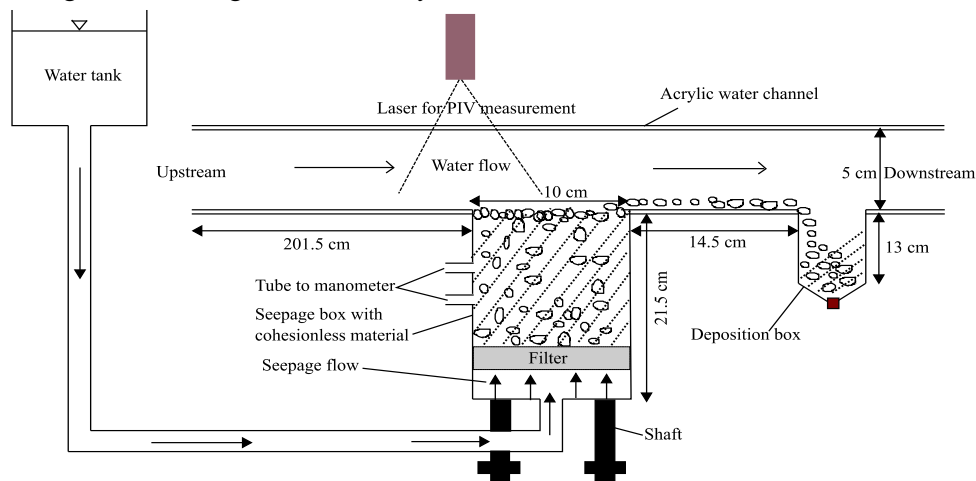


Fig. 2. Test apparatus consisting of the main flow channel, sediment box with cohesionless sample subjected to upward seepage flow and deposition box.

The laboratory examination of seepage effect was carried out in an acrylic glass-sided re-circulating close conduit with dimensions 10 cm in width, 5 cm in depth and 300 cm in length. The test apparatus for the experiment is shown in Fig. 2. Black silica sand particles with the mean diameter of 0.58 mm and the grain density of 2.64 g/cm<sup>3</sup> were used as the test material and packed in a sediment box at the bottom of the channel as shown in Fig. 2. A water tank was connected to the sediment box so that the test material was subjected to the upward seepage flow by lifting up the water tank. The deposition box was installed at the 14.5 cm downstream of the sediment box. The sediment particles transported along the water channel dropped in the deposition box. The weight of the deposited particles was measured and the sediment discharge rate was calculated for determining the critical tractive force of the test material. The structure of the test apparatus is similar to the EFA (Erosion Function Apparatus) of Briaud et al. (2001) while it did not include the water tank generating seepage flow and the deposition box.

The velocity measurement was conducted by the Laser-PIV technique. The friction velocity,  $u_*$  was calculated by curve fitting of the measured velocity

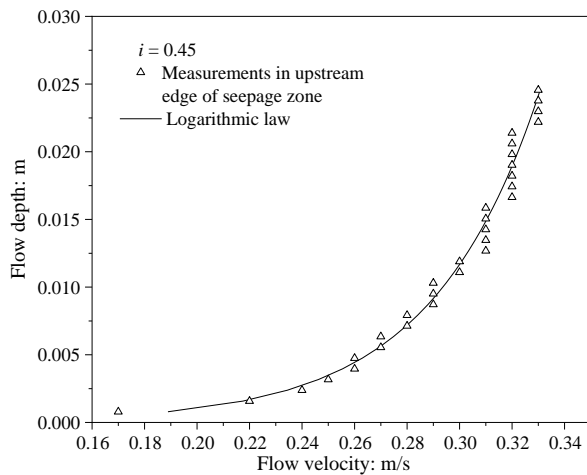


Fig. 3. Curve fitting of velocity profile to Logarithmic law and Modified logarithmic law.

profile to the logarithmic law in the upstream edge of seepage zone shown in Fig. 3.

$$u^+ = \frac{1}{k} \ln y^+ + A_s \quad (7)$$

$$u^+ = \frac{u}{u_*}, \quad y^+ = \frac{u_* y}{\nu} \quad (8)$$

where  $u$ ,  $u_*$ ,  $y$ ,  $\nu$ ,  $\nu$  and  $K$ ,  $A_s$  denote the horizontal flow velocity, the friction velocity, the vertical coordinate with its origin at the bed, the seepage velocity, the kinematic viscosity of water and the coefficients ( $K =$

0.41,  $A_s = 5.29$ ). The friction velocity,  $u_*$  is related to the bed shear stress,  $\tau$  as follows,

$$\tau = \rho_w u_*^2 \quad (9)$$

### 3 RESULTS AND DISCUSSION

We describe the results of the relationship between the sediment transport rate of the sand particles and the friction velocity calculated by curve fitting to the logarithmic law, Eq. (7) under various hydraulic gradients of 0.00, 0.15, 0.25, 0.35, 0.45, 0.55, 0.65 and 0.75 in Fig. 4 and Fig. 5, respectively. Both figures show that sediment transport rate variations over friction velocity are small even when hydraulic gradients increased. The value of the friction velocity which induces the incipient motion of sediment particles can be obtained as the x-intercept of the approximate line of higher sediment rates and corresponding friction velocities. Letting  $u_{*cs}$  be the value of the x-intercept, the critical tractive force under the seepage flow is calculated as,

$$\tau_{cs} = \rho_w u_{*cs}^2 \quad (10)$$

The value next to the vertical dash line in Fig. 4 and

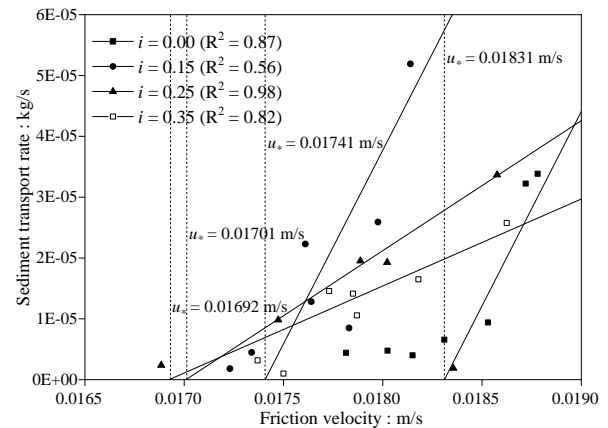


Fig. 4. Relationship between sediment transport rate of sand particles and friction velocity under the hydraulic gradients of 0.00, 0.15, 0.25 and 0.35.

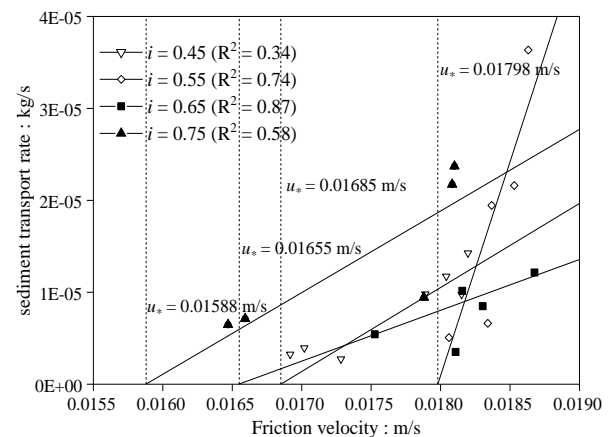


Fig. 5 Relationship between sediment transport rate of sand particles and friction velocity under the hydraulic gradients of 0.45, 0.55, 0.65 and 0.75.

Fig. 5 corresponds to the friction velocity at incipient motion. This method for determining the critical tractive force can avoid the subjectivity involved with the visual judgment of the incipient motion. Correlation and ordinary regression analyses were conducted to examine the relationship between friction velocity and sediment transport rate prediction. As can be seen each of the R-squared value for different hydraulic gradients is positively and significantly correlated. The sediment transport rate is linearly and incrementally dependent on friction velocity. The friction velocity value varies in a short range for different hydraulic gradients. So the friction velocity determined using x-intercept of an approximate line for different hydraulic gradients which causes incipient motion crosses each other for most of the observations shown in Fig. 4 and Fig. 5, respectively. Therefore, the dimensionless critical tractive force value for different hydraulic does not vary significantly. The relationship between the dimensionless critical tractive forces of the sand particles and the hydraulic gradients of 0.00, 0.15, 0.25, 0.35, 0.45, 0.55, 0.65 and 0.75 is shown in Fig. 6. It is seen from Fig. 6 that the dimensionless critical tractive force does not decrease with the increase of the hydraulic gradient as much as expected by Eq. (5) (The black solid line in Fig. 6 corresponds to Eq. (5)). The following reasons for the discrepancy between the value of the dimensionless critical tractive force in the upstream edge of seepage zone and Eq. (5) can be considered.

1. The hydraulic gradient on the bed surface is smaller than that in the bed, as was indicated by (Martin & Aral, 1971)
2. The bed shear stress was determined by the approach velocity profile at the upstream edge of the sediment bed, where the channel bottom is not permeable. The injection of the permeable sediment bed might significantly decrease the bed shear stress on it.

#### 4 CONCLUSION

The theoretical analysis and the experimental study

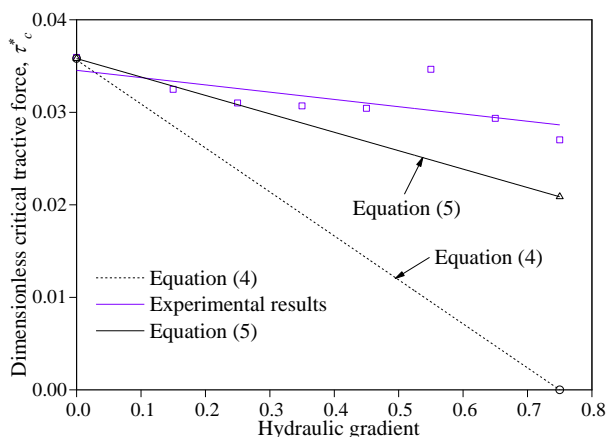


Fig. 6. Relationship between dimensionless critical tractive force and hydraulic gradient.

were conducted to investigate the critical tractive force of the sand particles under injection. Since the upward seepage force decreases the virtual weight of the bed material, the conventional concept of the dimensionless critical tractive force has shown that the induced upward hydraulic gradient decreases the critical tractive force linearly and does not diminish even it at the quicksand condition due to reduction of seepage force at bed surface as half as at several layers thick (Martin and Aral, 1971). The experimental results have revealed that the dimensionless critical tractive force acting on the cohesionless sand particles decreases slightly as the hydraulic gradient of the seepage flow increases when critical tractive force determined in the upstream edge of seepage zone. The linear fit line of the experiment lies above the line calculated by Eq. (5). Finally, we conclude that the critical tractive force of the cohesionless sand particles calculated in the upstream edge of seepage zone is a kind of maximum force.

#### ACKNOWLEDGEMENTS

The author would like to express his gratitude to Japanese Government for providing fully funded MEXT scholarship for two years Master's course study.

#### REFERENCES

- Briaud, J.L, Ting, F.C.K., Chen, H.C., Cao, Y., Han, S.W., and Kwak, K.W. (2001). Erosion function apparatus for scour rate predictions, *Journal of Geotechnical and Geoenvironmental Engineering*, 127(2), 105-113.
- Cao, D., Chiew, Y., and Yang, S. (2016). Injection effects on sediment transport in closed-conduit flows, *Acta Geophysica*, 64 (1), 125-148.
- Cheng, N-S., and Chiew, Y-M. (1998). Turbulent open-channel flow with upward seepage, *J. Hydraul. Res.*, 36(3), 415-431.
- Cheng, N-S., and Chiew, Y-M. (1999). Incipient sediment motion with upward seepage, *Journal of Hydraulic Research*, 37(5), 665-681.
- Dey, S., and Nath, T.K. (2010). Turbulence characteristics in flows subjected to boundary injection and suction, *Journal of Engineering Mechanics*, 136(7), 877-888.
- Dey, S., and Zanke, U.C.E. (2004). Sediment threshold with upward seepage, *J. Eng. Mech. ASCE* 130, 9, 1118-1123.
- Kavcar, P.C., and Wright, S.J. (2009). Experimental results on the stability of non-cohesive sediment beds subject to vertical pore water flux, In: *Proc. World Environmental and Water Resources Congress 2009: Great Rivers* 342, 3562-3571.
- Krogstad, P.Å., and Kourakine, A. (2000). Some effects of localized injection on the turbulence structure in a boundary layer, *Physics of Fluids*, 12(11), 2990-2999.
- Liu, X., and Chiew, Y.M. (2012). Effect of seepage on initiation of cohesionless sediment transport, *Acta Geophysica*, 60(6), 1778-1796.
- Lu, Y., Chiew, Y.M., and Cheng, N.S. (2008). Review of seepage effects on turbulent open-channel flow and sediment entrainment, *Journal of Hydraulic Research*, 46(4), 476-488.
- Martin, C.S., and Aral, M.M. (1971). Seepage force on interfacial bed particles, *J. Hydrol. Div., HY* 7, 1081-1100.